⊙ 研究論文

Fully Developed Turbulent Flow and Heat Transfer in Concentric Annuli with Surface Roughness

S. W. Ahn* · H. J. Kim*

표면거칠기가 있는 이중관내 완전히 발달된 난류유동과 열전달

안 수 환* · 김 형 진*

Key Words : roughness pitch(조도 피치), friction factor ratio(마찰계수비), heat transfer ratio (열전달비).

요 약

동심 이중관내에서 사각돌출형 조도요소에 의한 비대칭 난류유동과 열 전달 특성을, 열전달과 마찰계수에 미치는 조도의 합성효과를 조사하기위해, 연구하였다. 이론해석에서는 한쪽면에 거칠기가 있는 평행평판의 유동에 대한 수정 플란틀 혼합길이(mixing length)이론의 난류모델을 속도분포와 마찰계수를 구하는데 사용하였다. 최대속도지점에서 안쪽과 바깥쪽의 두 속도형상들은 힘의 평형에 의해 매치(match) 시켰다. 그리고나서, 온도 분포와 열전달 계수를 계산하였다. 속도형상과 마찰계수들의 해석 결과는 실험과 매우 잘 일치하였다. 마찰계수와 Nusselt number 에 미치는 조도비, 조도에 대한 피치비, 그리고 반경비등과 같은 여러 변수들의 효과들을 조사하였다. 본 연구는 일정 임의의 조도 요소들이 전체적 효율 측면에서 볼때 유리하게 열전달을 향상시킨다는 것을 증명하였다.

Nomenclature(see also Fig. 1)

a	thermal diffusivity
C	constant, 5.52
K	mixing length constant
De	equivalent diameter
P	pitch, between tips of roughness elements
Pr_t	turbulent Preandtl number
q	heat flux
R_j^+	$R_j(\tau_{Ro}/\rho)^{0.5}/\nu$
S	$R_o - R_i$
T_j^+	$(T_{Ri} - T_j)C\tau_{Ro}/[q_{Ri}(\tau_{Ro}/\rho)^{0.5}]$
U_j^+	$U_j/(\tau_{Ro}/\rho)^{0.5}$
y_j^+	$U_j(\tau_{Ro}/\rho)^{0.5}/\nu$
Z_{Ro}	imaginary location where $U_j=0$
α	radius ratio, R_i/R_o
δ_j	$\mid R_m - R_j \mid$
Δ	δ_j^+/R_j^+
ε	eddy diffusivity ; roughness height
ζ_j	y_j^+/δ_j^+

* 정회원, 통영수산전문대학

Subscripts :

H	Heat
i	inner
j	i or o
m	corresponding to the location of maximum velocity
M	momentum
o	outer
R	radius
r	rough
s	at sublayer boundary ; smooth
t	turbulent

1. Introduction

The flow in annular ducts has received considerable attention and it appears often in many areas of the thermal process industries and in fluid flow equipment. An annular geometry has long been recognized as an important flow channel employed for the design of heat exchangers and fuel burners. In nuclear engineering, it has served as a basic geometry in evaluating the heat transfer performance of various type of reactor elements including, in addition to single ribbed pins in a smooth cylinder, also more complex geometries such as rod bundles in circular or non - circular channels. Annulus flow is an axisymmetric geometry which, in the limiting cases, is reduced to the circular pipe and plane channel. For this reason, it has attracted the attention of researchers in the hope that its analysis would elucidate some of the evident difference between these two basic flow situations. In heat exchangers with enhanced heat transfer surfaces, surfaces which are sufficiently rough will have increased heat transfer coefficients because the turbulence setup in the wake of each roughness element will penetrate into the laminar sublayer. Therefore, it is generally expected that the effect would be greater for fluid with a higher Prandtl number. For the completely rough region in duct follow with relatively coarse and tightly spaced roughness elements, the friction factor is shown to be independent of the Reynolds number. Since the roughness of the surface not only increases the heat transfer rate, but also produces additional pressure losses, the heat transfer per unit pumping power expended may not be improved. Therefore, it is desirable to obtain optimum or advantageous geometrical shapes and arragements of the surface roughness elements. The patterns and effects of surface roughness on turbulent flow can not effectively described by any single parameter, such as the average roughness size (ε). Nevertheless many studies proceeded as if the average roughness size (ε) alone were sufficient to describe the flow induced by the surface roughness.

Schlichting[1] introduced the concept of equivalent sand grain roughness, K_s, as means of characterizing different types of surface roughness by referring to the equivalent net effect produced by Nikuradse's experiments, which were carried out in pipes that were artificially roughened with uniform grains of sand. Some other attempts[2,3] have been made to set up models of turbulent flow over rough surfaces.

Unfortunately, all these models require a prior knowledge of the function to describe a particular set of shapes and arragements of surface roughness elements. For such cases, there seems to be no reliable prediction for momentum and heat transfer available in the literature.

In our previous co - worker's report[4], a different approach from these models was used to indirectly describe a particular surface roughness for the prediction pressure loss and heat

transfer rate in an asymmetric flow induced by the given roughness elements. This approach was taken because, with asymmetric boundaries, the flow exhibits some characteristic aspects by virtue of symmetry that have been hidden.

In this study, it is assumed that the surface roughness affects only locally on the velocity profiles and therefore an empirical roughness correlation previously obtained for the flow between two parallel plates with square - ribbed surface roughness elements on the one surface only[4] could be used in the analysis.

The resultant effect of artificial roughness is determined from a comparison of rough and smooth surface with regard to the heat transfer increase relative to the increase in pressure losses.

2. Analysis

Because of the type of the roughness on the wall and geometrical characteristic of the annulus, local flow mechanism in the vicinity of that wall may not fully satisfy any universal velocity profiles. The large scale of roughness may cause a flow recirculation in the wake zone of the roughness elements; thus, the governing equations are broken into smooth and rough sides. For the analysis, we introduce the following assumptions(see Fig. 1) :

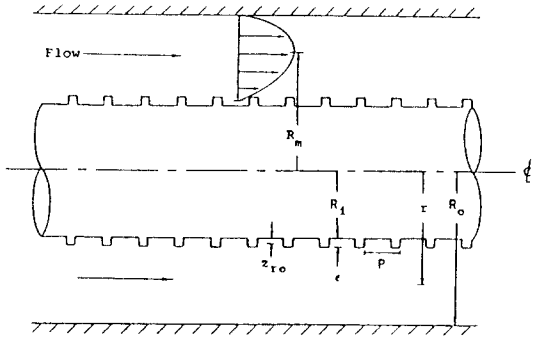

Fig. 1 Idealized Model

(i) The annuli is concentric. While the outer wall surface is smooth, the inner core surface is "square - ribbed".

(ii) Velocity and temperature fields in the annulus are fully developed.

(iii) The line of the maximum velocity coincides with the line of the zero shear stress.

(iv) For the smooth wall region, ε_M by van Driest[5] for the sublayer, and that of Reichardt[6] for the fully turbulent region are used.

(v) For the rough wall region, a modified logarithmic velocity profile is used. The surface roughness affects only locally on the velocity profiles.

(vi) The turbulent Prandtl number is taken unity.

2.1 Velocity and Temperature Distributions

For the velocity and temperature distributions, use is made of the concept of eddy diffusivity, ε_M and the turbulent Prandtl number, Pr_t. The basic equations governing the transport of momentum and heat can thus be written as :

$$\frac{\tau_j}{\rho} = (\nu + \varepsilon_M)\frac{\partial U_j}{\partial y} \qquad [1]$$

$$\frac{q}{c\rho} = (a + \varepsilon_H)\frac{\partial T}{\partial r} \qquad [2]$$

[1] can be non - dimensionalized as :

$$\frac{\partial U_i^+}{\partial \zeta_i} = \frac{U\tau_{Ri}}{U\tau_{Ro}}\frac{1}{K_i\zeta_i} \qquad \left(\frac{Z_{ro}^+}{\delta_i^+} < \zeta_i < 1\right) \qquad [3]$$

and

$$\frac{\partial U_o^+}{\partial \zeta_o} = \delta_o^+\left[\frac{(\tau/\tau_R)_o}{1+(\varepsilon_M/\nu)_o}\right] \quad (0 < \zeta_o < 1) \qquad [4]$$

where from a force balance. the shear stress distribution is :

$$\left(\frac{\tau}{\tau_R}\right)_i = \frac{(1-\zeta_i)[2+\Delta_i(1+\zeta_i)]\left(1+\Delta_i\frac{Z^+_{Ro}}{\delta^+}\right)_i}{(1+\Delta_i\zeta_i)\left[2+\Delta_i\left(1+\frac{Z^+_{Ro}}{\delta^+_i}\right)\right]\left(1-\frac{Z^+_{Ro}}{\delta^+_i}\right)} \quad [5]$$

and

$$\left(\frac{\tau}{\tau_R}\right)_o = \frac{(1-\zeta_o)[1-\Delta_o\zeta_o/(2-\Delta_o)]}{[1-\Delta_o\zeta_o]} \quad [6]$$

The initial conditions for [3] and [4] are : $U_i^+ = 0$ at $\zeta_i=(Z_{Ro}^+/\delta_i^+)$ and $U_o^+=0$ at $\zeta_0=0$. From [1] and [2], we can also obtain the following expressions[7] :

$$\frac{\partial T_j^+}{\partial \zeta_j} = \frac{\partial U_j^+}{\partial \zeta_j}\frac{\left(1+\frac{\varepsilon_M}{\nu}\right)(q_j/q_{Ri})}{\left(\frac{1}{\mathrm{Pr}}+\frac{1}{Pr_t}\frac{\varepsilon_M}{\nu}\right)(\tau/\tau_{Ro})_j} \quad [7]$$

where the heat flux distributions, from an energy balance, are :

$$\frac{\partial T_j^+}{\partial \zeta_j} = \frac{\partial U_j^+}{\partial \zeta_j}\frac{\left(1+\frac{\varepsilon_M}{\nu}\right)(q_j/q_{Ri})}{\left(\frac{1}{\mathrm{Pr}}+\frac{1}{Pr_t}\frac{\varepsilon_M}{\nu}\right)(\tau/\tau_{Ro})_j} \quad [8]$$

and

$$\frac{q_i}{q_{Ri}} = \frac{(1-\alpha^2(1+\Delta_i\zeta_i)\left(1+\Delta\frac{Z^+_{Ro}}{\delta^+}\right)_i}{\left[1-\alpha^2\left(1+\Delta_i\frac{Z^+_{Ro}}{\delta_i}\right)^2\right](1+\Delta_i\zeta_i)} \quad [9]$$

The initial conditions for [7] are :

$T_i^+=0$ at $\zeta_i=(Z_{Ro}^+/\delta_i^+)$.

The dimensionless velocity and temperature distributions in the inner and outer regions of the maximum velocity(see Fig. 1) can be obtained by solving these differential equations, [3], [4] and [7], once the eddy diffusivities and the matching conditions are established.

2.2 Eddy diffusivity for Momentum, ε_M.

Accuracy of description of the eddy diffusivity for momentum along and across the duct is required for a solution of velocity and temperature profiles. The most interesting feature of the study on turbulent fluid flow in a concentric annular duct is the complete failure in application of the conventional universal velocity profile or the law of wall[5]. Since the assumption of an eddy diffusivity of zero at the pipe line is not realistic, we postulate that Reichardt's expression[6] for the eddy diffusivity of momentum can be applicable to the entire turbulent flow regions on the outer smooth wall region of the concentric annulus with proper modification for the region remote from the outer wall. Thus, using the dimensionless parameters, we can obtain as follows :

For sublayer, $(0<y_o^+<y_{os}^+)$:

$$(\varepsilon_M/\nu)_o = K_o^2 y_o^{+2}[1-\mathrm{EXP}(-y_o^+/A_o^+)]^2\left|\partial U_o^+/\partial y^+\right| \quad [10]$$

For fully turbulent layer, $(y_{os}^+<y_o^+<\delta_o^+)$:

$$(\varepsilon_M/\nu)_o = [(K_o^+\delta_o^+)/6][1-(1-y_o^+/\delta_o^+)^2] \; X[1+2(1-y_o^+/\delta_o^+)^2] \quad [11]$$

And for the rough region, $(Z_{Ro}^+<y_i^+<\delta_i^+)$:

$$(\varepsilon_M/\nu)_i = (K_i^2 y_i^{+2})\left|\partial U_i^+/\partial y_i^+\right| \quad [12]$$

where

$$U_i^+ = (U\tau_{Ri}/U\tau_{Ro})(1/K_i)ln\frac{y_i^+}{Z^+_{Ro}} \quad [13]$$

and

$$Z_{Ro} = y_{mr}\mathrm{EXP}[-(U\tau_{Ro}/U\tau_{Ri}) \times\{ln(S-y_{mr})U\tau_{Ro}/\nu+CK_o\}] \quad [14]$$

and from the experimental study of Bhuiyan[8] :

$$y_{mr} = 0.299\, S\, Re^{0.066}(S/\varepsilon)^{0.14}(P/S)^{0.201} \quad [15]$$

2.3 Reynolds Number, Friction Factor and Nusselt Number.

Now that the eddy diffusivities(ε_M/ν) are known for the entire fluid region, the velocity and temperature profiles can be derived. The Reynolds number, friction factor, heat transfer coefficient and Nusselt number can be obtained in the usual way.

Reynolds number is defined as :

$$Re = U_b 2(R_o - R_i)/\nu = 2U_b^+(R_o^+ - R_i^+) \quad [16]$$

In dimensionless parameters, the average velocity(U_b) can be expressed as :

$$U_b = (\nu/R_o)\left[\frac{2\alpha}{1-\alpha^2}\right]\left[\delta_i^+ \int_{(Z_{Ro}/\varepsilon_i^+)}^{1}(1+\Delta_i\zeta_i)U_i^+ d\zeta_i + \frac{1}{\alpha}\delta_o^+ \int_0^1 (1-\Delta_o\zeta_o)U_o^+ d\zeta_o\right] \quad [17]$$

Friction factor in a dimensionless form from the usual definition yields :

$$f = 8\left\{\frac{(1-\alpha)^2\left[1+\frac{\alpha\tau_{Ri}}{\tau_{Ro}}\right]}{(1+\alpha)}\right\}\left(\frac{R_o^+}{Re}\right)^2 \quad [18]$$

From the definition, Nusselt number is :

$$N_u = \frac{2h(R_o-R_i)}{k} = 2\left[\frac{1-\alpha}{\alpha}\right]\frac{R_i^+ Pr}{T_b^+} \quad [19]$$

where $h = q_{Ri}/(T_{Ri} - T_b)$

The bulk temperature(T_b) can be defined in dimensionless parameters as :

$$T_b^+ = \left[\frac{4}{1+\alpha}\right]\left(\frac{1}{Re}\right)\left[\alpha\delta_i^+ \int_{(Z_{ro}^+/\delta_0^+)}^{1}(1+\Delta_i\zeta_i)U_i^+ T_i^+ d\zeta_i + \delta_o^+ \int_0^1 (1-\Delta_o\zeta_o)U_o^+ T_o^+ d\zeta_o\right] \quad [20]$$

2.4 Matching Conditions

2.4.1 Shear stresses.

From a force balance shear stresses become :

$$\frac{\tau_{Ri}}{\tau_{Ro}} = \left(\frac{R_o}{R_i+Z_{Ro}}\right)\left[\frac{R_m^2-(R_i+Z_{Ro})^2}{R_o^2-R_m^2}\right] \quad [21]$$

2.4.2 Relationship between K_i and K_o.

It is well established that the standard universal velocity is not fully adequate for the inner velocity distribution of a concentric annulus[9,10]. Therefore, while a fixed value of 0.4 for K_o is taken, the value of K_i is to be calculated from the appropriate boundary conditions in the analysis of concentric annuli with smooth walls[11,12]. However, in the present study, it is assumed that the turbulence induced by the surface roughness on the inner core surface is such that the effect of the curvature on the values of K is negligibly small. Therefore, it is assumed that ;

$$K_i = K_o \quad [22]$$

2. 4. 3 Velocity.

From the continuity of velocities at the location of the maximum velocity, ($r = R_m$, or $\zeta_i = \zeta_o = 1$), the maximum dimensionless velocity position becomes :

$$U_{om}^+ = U_{im}^+ \quad [23]$$

2. 4. 4 Relationship between T_{im}^+ and T_{om}^+.

From the equality of temperature at the location of maximum velocity(i. e. $r = R_m$ or $\zeta_i = \zeta_o = 1$), the matched dimensionless temperature position between the inner and outer wall regions is :

$$T_{om}^+ = T_{im}^+ \quad [24]$$

and

$$\frac{\partial T_{im}^+}{\partial \zeta_i} = -\frac{\partial T_{om}^+}{\partial \zeta_o}\frac{\delta_i^+}{\delta_o^+} \quad [25]$$

2. 6 Calculation

To obtain the results for a given Reynolds number, first of all, a Reynolds number should

be given ; however, the Reynolds number is actually obtained from the velocity profile, and the velocity profile is obtained from the given Reynolds number.

Therefore, a two - dimensional iteration ethod is used : one is for the velocity, and the other is for the Reynolds number. For the initial guess, a dimensionless sublayer thickness (ζ_{sub}) is used, and the dimensionless sublayer thickness(ζ_{sub}) is the number between 0 and 1, so that R_o^+ and R_m^+/R_o^+ are the variables of Reynolds number.

With the guessed R_m^+/R_o^+, the velocity profile in the smooth and rough parts are obtained, where we use the 5 - point Gaussian quadrature integration method. At the maximum velocity position, we check the equality of velocity. With the condition that velocities of both parts are equal, the Reynolds number is calculated with the velocity profiles obtained from Simpson's integration method with the number of nodes equal to 5000. If the velocities are not equal, we reguess the value of R_m^+/R_o^+.

If the calculated Reynolds number is equal to the given Reynolds number, the velocity profile is obtained. Finally, the friction factor, temperature profile, bulk temperature, and Nusselt number are calculated. And we use the parameters in calculation as follows :

a) Input parameters

α=0.2, 0.4, 0.5, 0.8 and 0.9.

R_o^+=in terms of Re ; 10^4 to 10^5.

P_r=0.1, 0.72, 1.0, 7 and 30.

P/ε=2, 4, 8 and 16.

S/ε=9.7, 19.4 and 25.

Pr_t=fixed at one for this paper.

b) Fixed parameters

A_o^+=26(van Driest damping parameter)

y_{os}^+=26(sublayer thickness)

3. Experiments

As is seen in Fig. 2, the total dimension of the main apparatus is about 7.98 meters in length. Air is drawn through a flow measuring orifice into a settling chamber and then through a bell - mouthed contraction section into the test section by a blower located at the extreme downstream end. The settling chamber consists of filters, flow straighteners, and screens with temperature measuring devices also provided inside. The bell - mouthed section is machined from a plexiglas block 305×305×203mm and the blower fan is rated 8.5 cu.m/min at 510mm of water.

Along the annular test section, which consists of a 97.4mm I.D. outer tube with a 39.2mm O.D. core tube with of 1.5mm, provisions are made for the measurement of the position of the core tube relative to the outer tube, pressure drops, and for the detailed exploration of the velocity field at the various cross sections along the test section. A specially designed traversing mechanism carried the measuring instrument. With this mechanism, the relative radial displacement of a probe is measured within 0.025mm by electrical contact. The core tubes are supported at three locations by 3 - point carriers which allow for radial adjustments of the core tube. When the test sections were assembled and aligned, the concentricity of the core to the outer tube was checked. The eccentricity due to the lack of straightness of

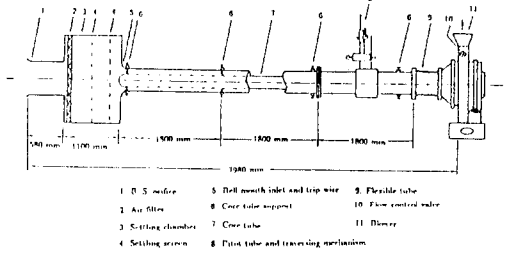

Fig. 2 Schematic diagram of experimental setup

the tubes was negligible in most cases, but a maximum of 2% was noted. The orifice of the flow rate measurement was calibrated by numerical integration of the velocity profiles measured at test sections. Steady state conditions were maintained for at least one - half hour before measurement were made. Pressure drop data were obtained over the entire accessible Reynolds number range whose upper limit was restricted by the blower capacity. Velocity profiles were explored with a total tube together with the static pressure taps provided on the outer tube of the annulus. The range of Reynolds number covered is from 15, 000 to 62,000 approximately. The pressure and temperature of the ambient are also recorded before each run. All the measurements are carried out only late in the night to avoid disturbances on the main power supply.

The main experimental variables for the present study are the pitch of the roughness(P) and the roughness height(ε) for each roughness pitch(P/ε=2, 4, 8), we take measurements of 1) static pressure drop versus channel length(x), 2) static pressure drop at fully developed conditions versus Reynolds number, 3) velocity profiles versus the radial location (y) using pitot tube at 78.9 equivalent diameters from the inlet of test tube, 4) double pitot tube reading the pressure difference versus the radial location (y) at fully developed conditions.

4. Results and Discussion

An example of predicted velocity profiles is compared with the experimental measurement in Fig. 3. In general the velocity profiles obtained through [3], [4] and by [13] agree reasonably well with the experimental data, except near the walls. The data for other ranges of parameters showed similar trend.

However, as can be seen in Fig. 4, these disagreements of the predicted velocity profiles from the experimental data did not greatly

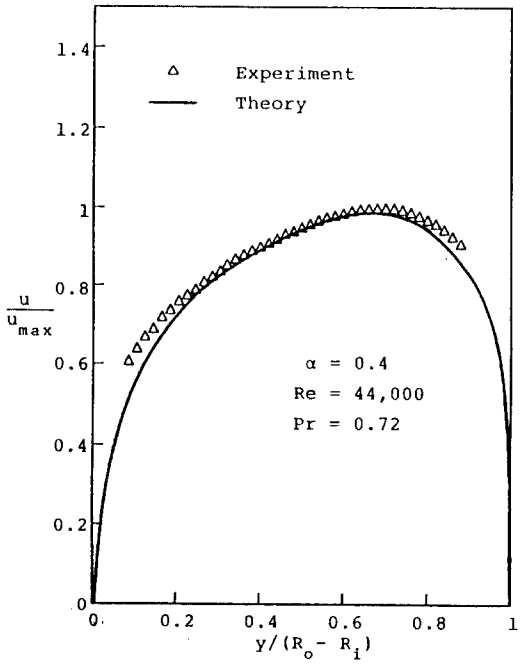

Fig. 3 Velocity distribution

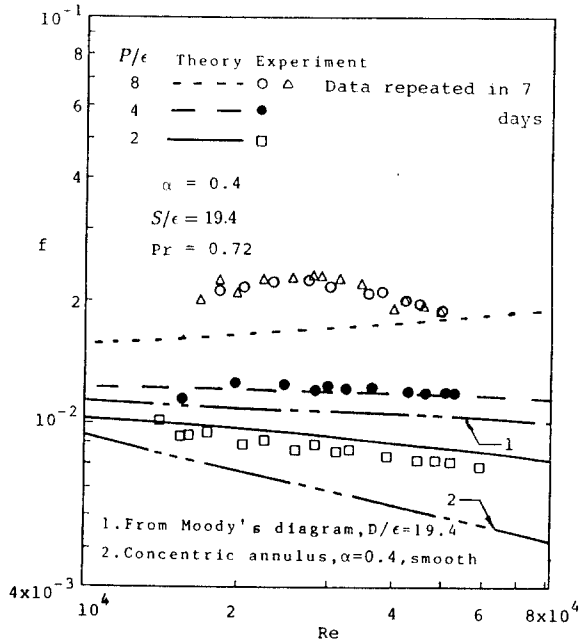

Fig. 4 Friction factor

affect the friction factors, which were predicted from these velocity profiles.

It seems that the deviation of the assumption used in the analysis diverges with increasing value of P/ε. It is obvious from the figure that the friction factor is strongly affected by the roughness density, P/ε. It was seen that f was also affected by the relative height of roughness, S/ε, as well as by the geometry of roughness elements. The figure also illustrates the deficiency of the Moody's diagram. In Fig. 5, the increase in pressure loss in terms of friction factor due to the roughness elements on the core tube is normalized by that of the smooth case. The normalized friction factor is defined as ;

$$F = f_r / f_s \qquad [26]$$

It can be seen that the effect of P/ε is significant. The effect of S/ε on F was also seen to be less, although the trend was opposite, that is, F decreases with increasing S/ε for the range of the parameters studied.

Heat transfer in terms of Nu was also normalized as :

$$H = Nu_r / Nu_s \qquad [27]$$

The effects of P/ε and Pr on H can be seen in Fig. 6 and the trends are similar to those observed in Fig. 5. The resultant effect of artificial roughness is determined from a comparison of rough and smooth surfaces with respect to the heat transfer increase relative to the increase in pressure losses. This is expressed in terms of a non - dimensional parameter, H/F, which is defined as :

$$H/F = (Nu_r / Nu_s)/(f_r / f_s) \qquad [28]$$

$H/F > 1$ suggests that the increase in heat transfer due to roughness is greater than the increase in pressure loss due to roughness and therefore it is advantageous to have the partic-

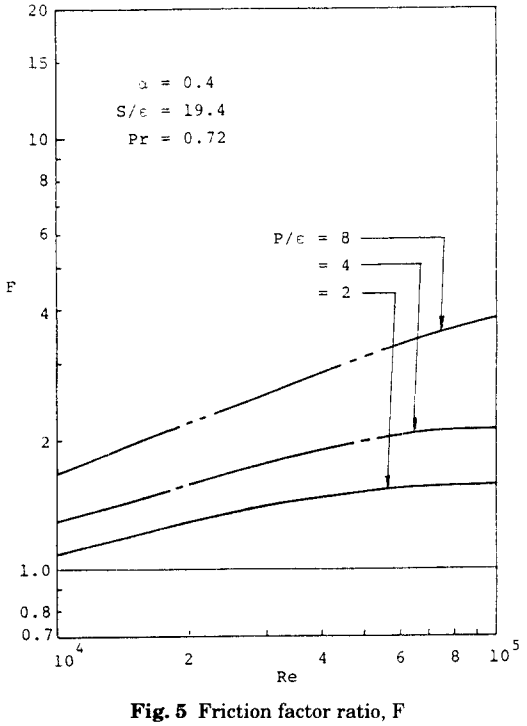

Fig. 5 Friction factor ratio, F

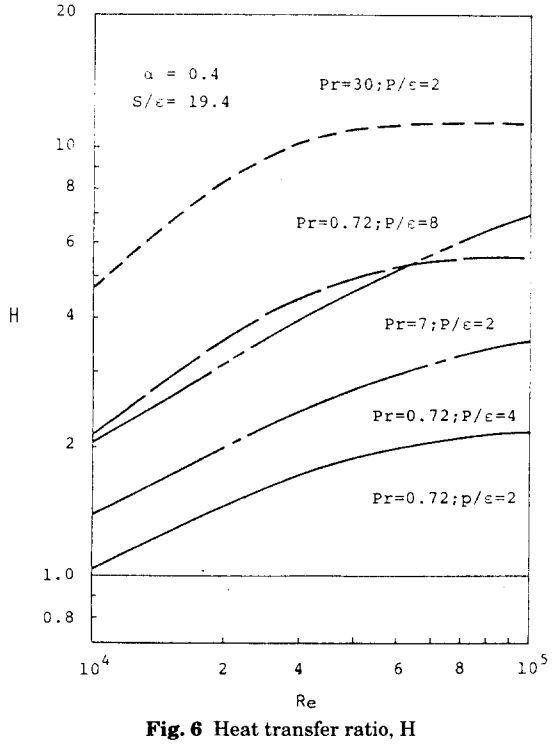

Fig. 6 Heat transfer ratio, H

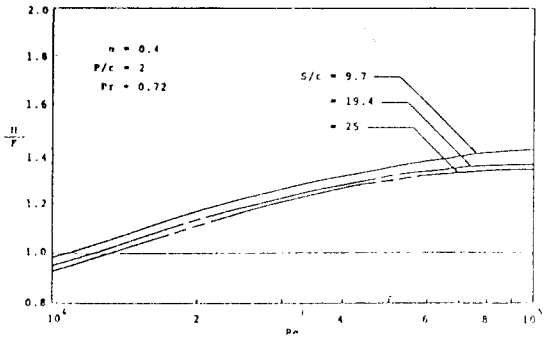

Fig. 7 Effects of Re and S/ε on H/F

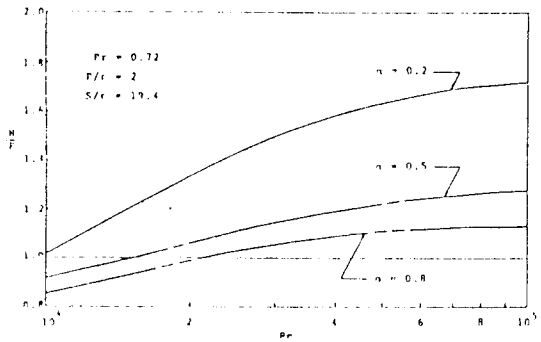

Fig. 8 Effects of Re and α on H/F

Table 1 H/F versus Pr and P/ε : theoretical
(α=0.4, S/ε=19.4, Re=50000)

P/ε	Pr	f_r	f_s	$F(f_r/f_s)$	Nu_r	Nus	$H(Nu_r/Nu_s)$	H/F
2	0.1	0.0087	0.0058	1.50	37.89	29.26	1.29	0.86
2	0.72	0.008	0.0058	1.50	204.77	107.78	1.90	1.27
2	1.0	0.0087	0.0058	1.50	277.97	132.08	2.10	1.40
2	10.0	0.0087	0.0058	1.50	2610.47	435.20	5.99	3.99
2	30.0	0.0087	0.0058	1.50	7789.19	670.11	11.62	7.75
4	0.1	0.0115	0.0058	1.98	51.14	29.26	1.75	0.88
4	0.72	0.0115	0.0058	1.98	310.89	107.78	2.28	1.45
4	1.0	0.0115	0.0058	1.98	427.61	132.08	3.24	1.64
4	10.0	0.0115	0.0058	1.98	4176.17	435.20	9.60	4.85
4	30.0	0.0115	0.0058	1.98	12505.74	670.11	18.66	9.42
8	0.1	0.0179	0.0058	3.09	85.21	29.26	2.91	0.94
8	0.72	0.0179	0.0058	3.09	557.60	107.78	5.17	1.67
8	1.0	0.0179	0.0058	3.09	770.54	132.08	5.81	1.89
8	10.0	0.0179	0.0058	3.09	7613.38	435.20	17.49	5.66

ular roughness elements from the overall efficiency point of view.

Fig. 7 shows the effects of Reynolds number and the relative height of roughness on H/F while Fig. 8 shows that of radius ratio for Reynolds number of 10,000 to 100,000. The ratio H/F increase greatly with decreasing radius ratio while there was a small increase in H/F with decreasing S/ε. The effect of increasing Reynolds number is the increase the ratio H/F.

The effect of Prandtl number on the ratio was not simple for the flow between two parallel plates with square - ribbed surface roughness elements on the one surface only[4] : H/F increased with increasing Prandtl number up to Prandtl number of about 10.

However, further increase in Prandtl number brought a decrease in H/F. In the present study, as can be seen in Table 1, an increase in Pr is always accompanied with an increase in H/F. The reason for the discrepancy between the two cases are not known for the moment.

5. Conclusion Remarks

From the analytical and experimental investigation on the drag force and heat transfer characteristics in the developed region of fluid flow flowing turbulently in concentric annulus with a uniformly heated core tube having square - ribbed surface roughness elements,

we can derive the conclusion that the effects of roughness density, relative roughness height, Reynolds and Prandtl numbers on the ratio H/F were identified for a turbulent flow induced by square - ribbed surface roughness elements on the core tube of a concentric annulus. The study demonstrates that certain artificial roughness elements can be used to enhance heat transfer rates with advantages from the overall efficiency point of view and that the required pumping power per unit heat transfer rate decreses with increasing value of P/ε, the decreasing values of S/ε and, α and increasing Reynolds and Prandtl numbers for the range of parameters studied.

Reference

1) Schlichting, H., 1968, "Boundary Layer Theory", 6th ed., McGraw Hill Book Co. Inc., pp. 578 - 589.
2) Allan, W.K. and Sharma, V., 1974, "An investigation of Low Turbulent Flows over Rough Surface", Jour. Mech. Eng. Sci.,Vol. 16, pp. 71 - 78.
3) Musker, A.J. and Lewkowicz, A.K., 1978,"The Effect of Ship Hull Roughness on the Development of Turbulent Boundary Layers", Proc. Int. Symposium on Ship Viscous Resistance, SSPA, Goteborg.
4) Lee, Y., 1987, "An Analysis on the Enhanced Heat Transfer induced by Square - Ribbed Surface Roughness",Heat Transfer Sci. and Tech., Hemisphere Pub. Co., N.Y., pp.781 - 788.
5) van Driest, E. R.,1956, "On Turbulent Flow Near a Wall", J. of Aero. Sci., Vol.23, pp. 485.
6) Reichardt, H., 1951, "Vollstandige Darstellung der turbulenten Geschwindigekeitsverterilung in glatten Leitungen, Z. amgew. Mathematic und Mechanik, Vol. 31, pp. 208 - 219.
7) Ahn, S. W., 1990, "Turbulent Fluid Flow and Heat Transfer Induced by Square - Ribbed Surface Roughness in Concentric Annuli", M. A. Sc. Thesis, Dept. of Mech. Eng., University of Ottawa.
8) Bhuiyan, A., 1977, "An Asymmetric Turbulent Fluid Flow Induced Rectangular Ribbed Surface Roughness", M.A.Sc. Thesis, Dept. of Mech. Eng., University of Ottawa.
9) Brighton, J.A. and Jones, J.B., 1964, "Fully Developed Turbulent Flow in Annuli", Trans. ASME, J. Bas. Engng., Vol. 86, pp. 835 - 844.
10) Jonsson V.K. and Sparrow, A., 1965, "Experiments on Turbulent Flow Phenomena in Eccentric Annular Ducts", J. Fluid Mech.,Vol. 25, pp. 65 - 86.
11) Barrow, H., Lee, Y. and Roberts, A.,1965, "The Similarity Hypothesis Applied to the Turbulent Flow in An Annulus, Int. J. Heat and Mass Transfer, Vol. 8, pp. 1499 - 1505.
12) Y. Lee, 1968, "Turbulent Heat Transfer from the Core Tube in Thermal Entrance Regions of Concentric Annuli, Int. J. of Heat and Mass Transfer, Vol. 11, pp. 509 - 522.